A Simple Model of the Wind-Driven Tropical Ocean

P. J. PHLIPS*

Department of Atmospheric Physics, Clarendon Laboratory, Oxford University

(Manuscript received 14 November 1986, in final form 26 May 1987)

ABSTRACT

A simple analytic theory for some aspects of the wind-driven circulation in the tropical oceans is described. The nearly geostrophic subsurface currents and the pressure field are studied by means of a single-layer model. The flow is forced by the locally determined pattern of convergence and divergence in the wind-driven surface boundary layer. Simple zonally symmetric divergence patterns are used. The response consists of long, damped equatorial waves.

This mechanism is strong enough to account for the strength of observed currents, as well as for typical patterns. The model's response to a uniform easterly wind is a strong eastward current centered on the equator, with weaker westward currents to the north and south. The eastward current at the equator is due to a Kelvin wave coming from the western boundary to satisfy the mass flux condition there. The model's undercurrent shifts south in response to a southerly wind component also at the equator. A band of boundary layer divergence is associated with the intertropical convergence zone. In the model this causes a trough in the ocean pressure field, and therefore an eastward equatorial countercurrent on its southern side.

1. Introduction

Ever since the rediscovery earlier this century of the strong subsurface current at the equator there has been much interest in the description and modeling of equatorial currents. The interest increased further when it became clear that anomalous conditions in the tropical oceans could affect the weather around the globe for many months. The equatorial oceans are found to be largely wind driven, and anomalous winds cause anomalous sea surface temperatures, which in turn affect the atmospheric circulation. The models developed to describe the wind-driven equatorial circulation range from linear analytical models such as those of Lighthill (1969) and Cane and Sarachik (1976, 1977, 1979) with a simplified vertical structure to fully nonlinear numerical models such as that of Philander and Pacanowski (1980).

The upper tropical oceans are characterized by a well-mixed layer in which the strongest currents are found, which is bounded below by a sharp thermocline. Below the thermocline the currents and pressure gradients are much weaker. It would therefore appear that the circulation in the upper tropical oceans is well suited to being described by simple single-layer models. However, existing simple models, such as Yamagata and Philander (1985) have had only limited success, and often miss completely such an important feature as the equatorial undercurrent. In this paper, a model is presented which may be useful in describing the height field and the nearly geostrophic currents found below the surface wind-driven boundary layer.

Gill (1975) describes two basic ideas through which the wind is thought to drive the equatorial oceans. The first is that at and near the equator the easterly winds drive some water downwind. This raises the surface in the western part of the ocean, and the resulting pressure gradient drives an eastward current. The second idea is that "the westward wind produces an Ekman flux, which is directed away from the equator. At the same time, the pressure gradient set up in response to the wind produces a geostrophic flow towards the equator below the surface. Thus the region close to the equator may be expected to be one of strong upwelling." There appears to be a similar correlation between the equatorial countercurrent and the region of upwelling associated with the intertropical convergence zone.

The two basic ideas boil down to the same mechanism. In both there is a wind-driven boundary-layer flow. In both there is then the idea that the boundary layer flow may be divergent and hence change the mass and height fields. The pressure gradients thus set up cause currents which are also divergent, in order to compensate the boundary layer divergence.

This suggests that a fruitful approach for simple, linear models would be to split the flow into a wind-driven boundary layer flow and a pressure driven interior flow. To describe the interior flow all one needs then is the divergence of the boundary layer flow. This is, of course, exactly the approach used in models of the midlatitude wind-driven circulation.

* Present Address: Beheerseenheid van het Mathematisch Model, Ministerie van Volksgezondheid, Linieregimentsplein, B-8400 Oostende, Belgium.

Many authors have followed the approach of Lighthill (1969) where the wind effect appears as a body force distributed throughout the depth. Yamagata and Philander (1985) show the steady state response to such forcing, consisting of damped long, equatorially trapped waves. The solution has the expected eastward pressure gradient but misses out the eastward mass flux at the equator. Moreover, the patterns of convergence and divergence are completely wrong.

Cane (1979a,b) developed a model in which the subsurface flow is driven by up- and downwelling of the surface flow, as proposed above. He split the ocean into a moving upper layer and a deep and denser lower layer assumed to be at rest. The upper layer of constant density was divided into a surface layer of constant thickness driven by the wind stress acting as a body force, and a second layer of variable thickness driven by the upwelling and downwelling of the surface flow.

Cane (1979b) did numerical spinup calculations with both the nonlinear model and with a linearized version. The linearized model attains a steady state in which there is little motion in the subsurface layer and the uniform wind stress is balanced by a tilting of the ocean surface. The nonlinear solution was much more realistic, with a strong eastward undercurrent at the equator, and westward currents to the north and south. Moreover, the nonlinear solution was more damped, in the sense of reaching a steady state after fewer oscillations.

The unrealistic linear solutions and the faster damping of the nonlinear solution can be explained using the results for damped long waves of Yamagata and Philander (1985). In the governing equations for the long waves they have damping terms $-\epsilon u$ in the zonal momentum equation, and $-\eta\phi$ in the combined continuity and thermodynamic equation. They show that the damping of the waves is proportional to $(\epsilon\eta)^{1/2}$, and that the meridional extent of the flow and the ratio of potential to kinetic energy both increase as ϵ/η increases. The linear solutions of Cane (1979b) correspond to the limit $\eta \to 0$, as there was no damping term in the continuity equation, and are well explained by the theory of Yamagata and Philander.

The present model is described in the next section. Rather than separate the upper layer into two sublayers, the dependent variables are divided between a wind-driven boundary layer and a pressure-driven flow. A solution for the pressure-driven flow is obtained in terms of the divergence of the wind-driven boundary layer flow. To provide a self-contained description of the wind-driven circulation, and in particular of the surface velocities, one therefore needs to combine the present model with a boundary layer model.

In section 3 an analytic solution is obtained for damped waves in an ocean bounded east and west by straight boundaries. In section 4 a particular solution for forcing symmetric about the equator is presented, such as might result from a uniform easterly wind. This simple case already displays the main features of the observed circulation, namely a strong, narrow eastward jet at the equator with weaker westward flow to the north and south, a surface sloping down towards the east at the equator, with much stronger ridges of high pressure in the tropics.

In section 5 the response to simple cases of asymetric forcing is presented. Meridional winds near the equator tend to shift the center of the undercurrent upwind, away from the equator. An intertropical convergence zone centered some distance from the equator causes a second narrow eastward jet, representing the North Equatorial Countercurrent, and a dip in the height field. It is found that if the preceding three forcing effects are combined, the linear analytic model is able to reproduce the important features of the northern summer circulation in the tropical Pacific Ocean.

In section 6 an even simpler analytic model is presented, where the equatorial waves were undamped and a very simple model of the boundary layer flow is used. When a uniform easterly wind is applied, this model reproduces the main features of the zonal velocity and pressure found in the model with damped waves. We therefore conclude that the main features of the tropical circulation can be explained by the combination of nearly geostrophic flow and boundary layer divergence, and are not due to nonlinearity, particular damping laws, or other effects. Finally, in section 7 the model is compared with the wind stress forcing formulation which is sometimes used.

2. The model

Whereas it seems clear and well established that the tropical circulation is largely driven by the wind and that it is set up through the action of equatorially trapped waves, the point of how to model the mechanism whereby the wind excites the waves does not appear to have been settled. We propose that a useful way to model the flow is to split it into a wind-driven surface boundary layer and a pressure-driven flow, which is nearly uniform throughout the depth of the upper layer. On the one hand, this method is not new inasmuch as this physical mechanism is just the same as for the midlatitude wind-driven circulation, and corresponds to that of some other models, such as the two-layer nonlinear model of Cane (1979b). On the other hand, the model is new inasmuch as the present formulation does not appear to have been used before to describe the equatorial wind-driven circulation. The present method allows a very simple description of the mechanism whereby the wind forces the equatorially trapped waves. To put it succinctly, the equatorial waves are forced by the divergence of the flow in the surface boundary layer, which is itself forced directly by the local wind.

First we shall review why the flow can be separated into a boundary-layer and a pressure-driven flow. Typ-

ical profiles of zonal velocity and density near the equator are sketched in Fig. 1. Since the density is nearly uniform throughout the depth of the upper layer, it follows that the pressure too is nearly uniform throughout the depth of the upper layer. This in turn implies that the flow associated with the pressure gradient will be nearly uniform throughout the depth of the upper layer. The profile of zonal velocity, on the other hand, shows a strong shear at the surface, decreasing as one goes down, with a second region of strong shear at the base of the thermocline. Farther down the zonal velocities are much smaller. The velocity shear at the base of the thermocline is associated with the changes in the pressure gradient there, but the shear near the surface cannot be related to pressure forces. As previously argued, the pressure gradients would tend to induce velocities uniform throughout the upper layer. The velocity shear near the surface is therefore in direct response to the wind stress applied at the surface. These two features, namely a strong shear near a free surface where a stress is applied, and a pressure which varies little through the region of strong shear, practically constitute a definition of a boundary layer.

It follows that one can divide the upper-layer velocity field into a part which is related to the pressure gradient and therefore approximately independent of depth in the upper layer, and a boundary-layer flow related to the surface wind stress, with strongest velocities at the surface and strong shear. This split is not only kinematic but also dynamic, since large-scale pressure gradients are a major item in the balance of forces for the first component but not for the second, whereas turbulent Reynolds stresses are a major item for the second but not for the first.

Another consequence of the preceding argument is that the stress applied at the surface does not project uniformly throughout the upper layer, but is taken up more strongly near the surface by the shear and turbulence associated with the surface boundary layer. One cannot, therefore, expect a direct balance between wind stress and pressure gradient at each point on the ocean surface.

Circulations consisting of a pressure-driven flow and a surface boundary layer can also be seen in other models. These models may be classified according to the amount of vertical resolution they provide: single-layer models with wind stress forcing (Cane and Sarachik, 1976, 1977, 1979; Yamagata and Philander, 1985), two-layer models (Cane 1979a, 1979b), and continuous models (McCreary, 1981; McPhaden, 1981). In the continuous models one solves for the boundary layer and pressure driven parts of the circulation simultaneously, but the two parts can still be clearly distinguished. In a latitude/depth section of McCreary's solution, for example, one can clearly see that the surface flow at the equator is poleward and divergent, whereas the subsurface flow is equatorward and convergent.

The two-layer nonlinear model of Cane (1979b) also provided a realistic set of currents and height field. In this model, the mixed layer of the ocean was split into two layers, with the wind stress acting as a body force in the upper layer. The governing equations for this model were nonlinear and solved numerically. Cane showed that the pressure in the two layers is nearly the same. It follows that the difference between the upper and lower-layer velocities is due to the wind force in the upper layer.

The velocity difference is therefore a simple representation of the boundary-layer flow. Since the upper-level flow is divergent, the pressure-driven flow must have a compensating convergence. We see, therefore, that Cane's model also contains the mechanism of a divergent boundary layer driving the subsurface flow, but the central importance of this mechanism is, perhaps, masked by the complications arising from the presence of two layers, nonlinearity, and a numerical method of solution. In this paper we shall establish the importance of the boundary-layer divergence forcing by obtaining essentially similar circulations with this forcing in single-layer, linear, analytic, damped, and inviscid models.

The single-layer models in which the wind stress acts as a body force distributed over the upper layer have not been very successful at describing the steady state

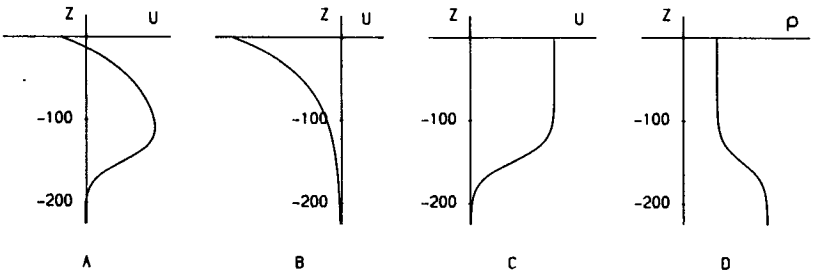

FIG. 1. Sketch of a typical velocity profile at the equator (A). This is taken to be the sum of a wind-driven surface boundary layer (B), and a pressure-driven flow (C). The pressure-driven flow is nearly uniform down to the thermocline because the upper layer is well mixed (D).

flow. With these models the main response to a uniform zonal wind is limited to a sloping surface over the whole basin, thus missing completely the typical equatorial current system and the dip in the surface height near the equator relative to the tropics. In view of the previous discussion it might seem that the single-layer model misses a large part of the observed features of the tropical ocean because, by definition, it does not include a surface boundary layer. A more detailed discussion in section 7 will show that the single-layer stress models are equivalent to models forced by boundary-layer divergence, but only if the boundary-layer mass flux can be described by the Ekman relation. This is not the case near the equator.

We shall now derive the equations for the present model. The model ocean has a simplified vertical structure with a moving upper layer of density ρ and depth h, and a deep lower layer at rest and with a density $\rho + \Delta\rho$. The pressure-driven flow is assumed to be small enough that nonlinear effects are fairly weak, so that in a simple model the equations may be linearized about a state of rest as a first approximation. In the absence of friction the momentum equations for the pressure-driven flow would then be

$$\frac{\partial u'}{\partial t} - \beta y v' = -\frac{1}{\rho}\frac{\partial p}{\partial x} \tag{1}$$

$$\frac{\partial v'}{\partial t} + \beta y u' = -\frac{1}{\rho}\frac{\partial p}{\partial y} \tag{2}$$

where u' and v' are the zonal and meridional pressure-driven velocities. The continuity equation for the upper layer is

$$\frac{\partial h}{\partial t} + \frac{\partial}{\rho x}(u'h + U_E) + \frac{\partial}{\partial y}(v'h + V_E) = 0 \tag{3}$$

where U_E and V_E are the zonal and meridional transports in the wind-driven boundary layer flow. The layer thickness h is the sum of its mean thickness H, the surface displacement ζ, and the thermocline displacement η. As the lower layer is at rest, the thermocline displacement is proportional to, and much larger than, the surface displacement,

$$\eta = -\frac{\rho}{\Delta\rho}\zeta, \quad \eta \gg \zeta. \tag{4}$$

If we work with the geopotential ϕ instead of surface displacement and pressure we have

$$\phi = g\zeta = p/\rho, \tag{5}$$

and the linearized equation may be written

$$\frac{\partial \phi}{\partial t} + c^2\left(\frac{\partial u'}{\partial x} + \frac{\partial v'}{\partial y}\right) = -\frac{\Delta\rho}{\rho} g\left(\frac{\partial U_E}{\partial x} + \frac{\partial V_E}{\partial y}\right), \tag{6}$$

where $c^2 = (\Delta\rho/\rho)gH$ and c is the speed of long internal gravity waves.

From now on the divergence of the boundary-layer flow will simply be considered as a known quantity W_E. Equations (1), (2) and (6) are nondimensionalized using, as length scale, the equatorial Rossby radius $a = (c/2\beta)^{1/2}$ and the corresponding time scale $(2\beta c)^{-1/2}$. With a wave speed O(2.5) m s^{-1}, the Rossby radius is O(250) km and the time scale O(1) day. The zonal velocity scale is given by $(a/H)\partial V_E/\partial y$. The divergence at the equator does not appear to be very well known, but typical estimates given upwelling velocities of the order of a few meters per day. If, for the sake of definiteness, we take $\partial V_E/\partial y \approx 3 \times 10^{-5}$ m s^{-1} and $H \approx 150$ m, then the zonal velocity scale is 5 cm s^{-1}.

The effects of friction and mixing may be represented most simply and crudely by linear damping laws; i.e., by replacing the time derivatives $(\partial/\partial t)$ by $(\partial/\partial t + \epsilon)$. Moreover, as the zonal scale of the motions is much longer than the meridional scale, we can make the long wave approximation (see Gill and Clarke, 1974; Gill and Phlips, 1986), so that the meridional momentum equation reduces to a geostrophic balance. With these scalings and approximations, (1), (2) and (6) become

$$\left(\frac{\partial}{\partial t} + \epsilon\right)u - \frac{1}{2}yv = -\frac{\partial \phi}{\partial x} \tag{7}$$

$$\left(\frac{\partial}{\partial t} + \epsilon\right)\phi + \frac{\partial v}{\partial y} = -\frac{\partial u}{\partial x} - W_E \tag{8}$$

$$\frac{1}{2}yu = -\frac{\partial \phi}{\partial y}. \tag{9}$$

The problem, as set up in (7)–(9), is now formally identical with the model of Gill (1980) for the atmospheric circulation driven by deep convection in the tropics. This model has been extensively studied; Gill (1980) and Gill and Phlips (1986) have given simple solutions and the basic dynamics, Heckley and Gill (1984) have studied the initial adjustment, and Gill and Phlips (1986) have looked at nonlinear effects. The formal similarity between the equations for the atmospheric large-scale circulation and the oceanic large-scale circulation is not a coincidence but results from the close similarities in the physics. Whereas in the oceanic case the divergence of the large-scale flow is forced by the boundary-layer divergence, in the atmospheric case the divergence of the large-scale flow is forced by mass transfer between the lower and upper atmosphere in deep convection. In both cases the forcing function is not a direct function of the large-scale flow variables, and can be externally specified in simple theoretical models.

3. Steady state solutions

In this section steady state solutions of the governing equations (7)–(9) will be obtained. It is found more convenient to work with new dependent variables q and r,

$$q = \phi + u, \quad r = \phi - u. \tag{10}$$

The sum and difference of (7) and (8) and (9) then become

$$\epsilon q+\frac{\partial q}{\partial x}+\left(\frac{\partial}{\partial y}-\frac{1}{2}y\right)v=-W_E \tag{11}$$

$$\epsilon r-\frac{\partial r}{\partial x}+\left(\frac{\partial}{\partial y}+\frac{1}{2}y\right)v=-W_E \tag{12}$$

$$\left(\frac{\partial}{\partial y}+\frac{1}{2}y\right)q+\left(\frac{\partial}{\partial y}+\frac{1}{2}y\right)r=0, \tag{13}$$

in the steady state. In (11)–(13) we see the index-raising and index-lowering operators for the parabolic cylinder functions $D(y)$ (Abramowitz and Stegun, 1965). These functions satisfy

$$\frac{dD_n}{dy}+\frac{1}{2}yD_n=nD_{n-1}, \quad \frac{dD_n}{dy}-\frac{1}{2}yD_n=-D_{n+1} \tag{14}$$

and the first three functions are

$$\begin{pmatrix}D_0\\D_1\\D_2\end{pmatrix}=\begin{pmatrix}1\\y\\y^2-1\end{pmatrix}\exp\left(-\frac{1}{4}y^2\right). \tag{15}$$

Equations (11)–(13) are found to have modal solutions,

$$\left.\begin{aligned}q&=q_{n+1}(x)D_{n+1}(y)\\v&=v_n(x)D_n(y)\\r&=r_{n-1}(x)D_{n-1}(y)\end{aligned}\right\}, \quad n=-1,0,1,2,\cdots, \tag{16}$$

where it is understood that quantities with a negative index are zero.

In order to be able to solve the problem, some specific assumptions about the distribution of the boundary layer divergence have to be made. It will be assumed that the divergence can be written in a separable form

$$W_E=F(x)\sum_{n=0}^{\infty}W_nD_n(y). \tag{17}$$

The observations of Wyrtki and Meyers (1976) show that the regions of boundary-layer divergence are confined to thin strips, mainly concentrated in the Pacific at the equator and near 10°N in July. As a first approximation in a simple model we shall take it that the regions of convergence and divergence are zonally symmetric, so that $F(x) = 1$, and W_E may be described by superposition of distributions

$$W_E=D_0[\alpha(y-y_0)], \tag{18}$$

where y_0 is the latitude of maximum divergence and α^{-1} determines the width of the region of divergence. This expression may be put (Phlips and Gill, 1986) in the form (17)

$$W_0=\left(\frac{2}{1+\alpha^2}\right)^{1/2}\exp\left(-\frac{1}{4}\frac{\alpha^2}{1+\alpha^2}y_0^2\right)$$

$$W_{n+1}=\frac{1}{n+1}\left[\left(\frac{1-\alpha^2}{1+\alpha^2}\right)W_{n-1}+\left(\frac{\alpha^2}{1+\alpha^2}\right)y_0W_n\right]. \tag{19}$$

If (11)–(13) are now separated into modes using (14), (16) and (17) we find

(i) Kelvin mode ($n = -1$)

$$\epsilon q_0+\frac{\partial q_0}{\partial x}=-W_0, \quad v=r=0. \tag{20}$$

(ii) Mixed mode ($n = 0$)

$$v_0=W_1, \quad q=r=0. \tag{21}$$

(iii) Planetary modes ($n \geqslant 1$)

$$(2n+1)\epsilon q_{n+1}-\frac{\partial q_{n+1}}{\partial x}=-(W_{n-1}+nW_{n+1}) \tag{22}$$

$$v_n=[W_{n-1}+(n+1)W_{n+1}]+2(n+1)\epsilon q_{n+1} \tag{23}$$

$$r_{n-1}=(n+1)q_{n+1}. \tag{24}$$

The particular solutions to these equations are simply

Kelvin mode:

$$q_0{}^F=-W_0/\epsilon. \tag{25}$$

Mixed mode:

$$v_0{}^F=W_1. \tag{26}$$

Planetary modes:

$$\begin{aligned}q_{n+1}^F&=-(W_{n-1}+nW_{n+1})/(2n+1)\epsilon\\v_n{}^F&=-[W_{n-1}-(n+1)W_{n+1}]/(2n+1)\\r_{n-1}^F&=-(n+1)(W_{n-1}+nW_{n+1})/(2n+1)\epsilon.\end{aligned} \tag{27}$$

To complete the solution it remains to satisfy the boundary conditions at the eastern and western ends of the basin. The boundaries are taken to be straight lines, the western boundary being defined by $x = 0$ and the eastern boundary by $x = L$.

At the eastern boundary the condition $u = 0$ gives the relation

$$q_{n+1}=q_{n-1}/(n+1) \quad \text{at} \quad x=L, \tag{28}$$

since the q and r are related by (24). For the mixed mode $q_1 = 0$, it follows by (28) that all the antisymmetric modes must be zero at $x = L$.

At the western boundary we also have the condition that the zonal velocity must be zero. But by making the long-wave approximation, we have filtered out of the governing equations the eastward-propagating short planetary waves making up the western boundary layer. As a result, we cannot satisfy the condition at the boundary itself, but we can assure that the effect of the boundary condition on the interior flow is satisfied. That is, the total mass flux normal to the boundary must be zero at the longitude of the boundary, $\int_{-\infty}^{\infty}u(0)dy = 0$, which gives

$$q_0=q_2+1\times(q_4+3\times(q_6+5\times(q_8+\cdots))) \quad \text{at} \quad x=0. \tag{29}$$

This gives the amplitude of the reflected Kelvin wave in terms of the incident planetary waves.

The free solutions of (20) and (22)–(24) needed to complete the solution are

(i) Kelvin mode:

$$\tilde{q}_0 = Q_0 \exp(-\epsilon x). \tag{30}$$

(ii) Planetary modes:

$$\tilde{q}_{n+1} = Q_{n+1} \exp[(2n+1)\epsilon(x-L)]$$
$$\tilde{v}_n = 2(n+1)\epsilon\tilde{q}_{n+1}$$
$$\tilde{r}_{n-1} = (n+1)\tilde{q}_{n+1}. \tag{31}$$

If (30) and (31) are used in (28) and (29) we find that the amplitude of the reflected Kelvin wave is given by

$$\left(1-\frac{1}{2}e^{-4\epsilon L}-\frac{1}{2\cdot 4}e^{-8\epsilon L}-\frac{3}{2\cdot 4\cdot 6}e^{-12\epsilon L}\right.$$
$$\left.-\frac{3\cdot 5}{2\cdot 4\cdot 6\cdot 8}e^{-16\epsilon L}\cdots\right)Q_0 = q_0{}^F\left(-1+\frac{1}{2}e^{-3\epsilon L}\right.$$
$$\left.+\frac{1}{2\cdot 4}e^{-7\epsilon L}+\frac{3}{2\cdot 4\cdot 6}e^{-11\epsilon L}+\frac{3\cdot 5}{2\cdot 4\cdot 6\cdot 8}e^{-15\epsilon L}+\cdots\right)$$
$$+q_2{}^F(1-e^{-3\epsilon L})+q_4{}^F(1-e^{-7\epsilon L})+3\cdot q_6{}^F(1-e^{-11\epsilon L})$$
$$+3\cdot 5\cdot q_8{}^F(1-e^{-15\epsilon L})\cdots, \tag{32}$$

and the amplitudes of the reflected symmetric planetary waves are given by

$$Q_2 = -q_2{}^F+\frac{1}{2}(q_0{}^F+Q_0e^{-\epsilon L})$$
$$Q_4 = -q_4{}^F+\frac{1}{2\cdot 4}(q_0{}^F+Q_0e^{-\epsilon L})$$
$$Q_6 = -q_0{}^F+\frac{1}{2\cdot 4\cdot 6}(q_0{}^F+Q_0e^{-\epsilon L}), \tag{33}$$

etc., whereas the amplitudes of the reflected antisymmetric waves are simply

$$Q_3 = -q_3{}^F, \quad Q_5 = -q_5{}^F, \quad Q_7 = -q_7{}^F. \tag{34}$$

This completes the solution.

4. Response to uniform easterly winds

The first result is for strong boundary-layer divergence at the equator with convergence to the north and south, which is much more spread out. Mathematically, we take

$$W_E = D_0(3y)-\frac{1}{9}D_0(y/3). \tag{35}$$

The integrated convergence and divergence are then equal. The pattern (35) is meant to represent the fact that for a uniform easterly wind the meridional Ekman flux goes from zero at the equator to a maximum a few hundred kilometers away from the equator, and then slowly decreases as one proceeds to higher latitudes.

The flow is shown in Fig. 2 for a damping constant $\epsilon = 0.01$ corresponding to a damping time of order of 100 days, a value chosen to give reasonable magnitudes for the velocities. The zonal and meridional distances are in Rossby radii. The length of the basin is 40 Rossby radii, which is of the order of 10^4 km. The lines are pressure contours and the arrows current vectors. The flow has a strong eastward current at the equator with weaker westward currents to the north and south. These westward currents are nearly geostrophic. The eastward undercurrent is also in geostrophic balance in the meridional direction. This implies that the meridional pressure gradient reverses near the equator, as can be seen from the Σ shaped equatorial contours in Fig. 2, or directly in the midbasin meridional section in Fig. 3. Figures 2 and 3 also show that the thermocline will be deepest in the western half of the basin, about four Rossby radii from the equator.

In the model the eastward current at the equator flows from high pressure to low, as is observed. This can be seen in Fig. 4, which is a zonal section along the equator. The eastward current and the pressure gradient go to zero at the eastern boundary [not exactly, because only a finite number of modes (38) is used in the calculation]. As the damping is reduced, the amplitudes of the pressure and velocities increase, although not quite inversely proportionally (Fig. 5). The flow pattern is unchanged, though. The strongest velocities in Figs. 2, 3 and 4 are about 70 cm s^{-1}, which is typical of observed speeds in the undercurrent. The magnitudes of the surface heights, on the other hand, are much smaller than are observed. This could easily be remedied by generalizing the model to have weaker damping in the continuity equation and stronger damping in the zonal momentum equation. It was shown by Yamagata and Philander (1985) that the only modification compared to the method of section 3 is that each variable has an additional scaling parameter in powers of the ratio of the two damping constants.

The pattern of eastward and westward currents may be explained by dynamical similarity with the atmospheric Hadley circulation. In the present model the subsurface flow is divergent away from the equator and strongly convergent at the equator. This is also found in the continuous models of McCreary (1981) and McPhaden (1981). It is also similar to the low-level branch of the Hadley circulation. Hadley argued that the equatorward motion would lead to easterly winds, or westward currents here. Since the eastward velocity of the earth's surface is higher at the equator than to the north and south, a parcel of water starting in the tropics and moving equatorward would find itself moving more slowly than the earth's surface. Relative to the earth's surface one would then observe westward currents.

Figure 6 shows meridional sections of pressure and velocity for the solution (25)–(27) in the absence of lateral boundaries. One finds westward currents in both

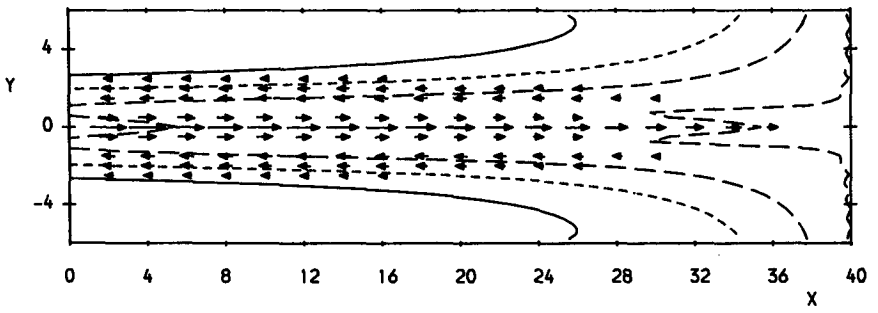

FIG. 2. Solution for symmetric forcing with boundary layer divergence at the equator and weak convergence to the north and south. Zonal and meridional distances are in Rossby radii O(250) km. The arrows are current vectors and the lines are pressure contours (solid contours positive, dashed zero, and broken negative) at intervals of ten units. The damping constant $\epsilon = 0.01$ corresponds to a damping time constant O(100) days. There is strong eastward flow at the equator, with weaker westward flow to the north and south. The equator is an area of low pressure throughout the basin, although at the equator itself the pressure drops towards the east.

hemispheres going to zero at the equator. It is interesting to imagine how such a flow is set up if the winds are suddenly "switched on" over an ocean at rest. The boundary layer divergence at the equator causes the surface to drop and the thermocline to rise there. Conversely, convergence away from the equator causes the surface to rise and the thermocline to deepen, as can be seen in Fig. 6. The resulting pressure gradients cause westward currents by geostrophy, both to the north and south of the equator. There is then a net zonal flow towards the western boundary, so that the surface will rise near the boundary. This in turn will cause an eastward, down-pressure current at the equator, also known as the reflected Kelvin wave, or as the equatorial undercurrent.

5. The response to asymmetric forcing

The components of the divergence forcing which are asymmetric about the equator can have an important effect on the currents and on the pressure and mass fields. Gill (1982) discusses two such situations. The first is where a southerly wind component at the equator causes boundary-layer divergence south of the equator, and convergence north of the equator. The equatorial undercurrent is found to move southwards in response to this. The second case concerns the equatorial countercurrent and the trough in the ocean pressure field around 10°N which appear to be associated with a region of boundary layer divergence, which, in turn, is associated with the intertropical convergence zone. We shall investigate how the model reproduces these features.

Away from the equator the Ekman mass flux associated with a southerly wind is zonal. At the equator, however, the boundary-layer mass flux will be downwind, i.e., northward. There will therefore be boundary-layer divergence just south of the equator, and equal and opposite convergence just north of it. We shall model this using a divergence distribution

$$W_E = -D_1(3y) = -3yD_0(3y), \tag{36}$$

so that the coefficients W_n can still be computed using (19). The resulting flow (Fig. 7) consists of a narrow eastward current south of the equator, and an opposite westward current north of the equator. The effect of a meridional wind is thus to shift the undercurrent up-

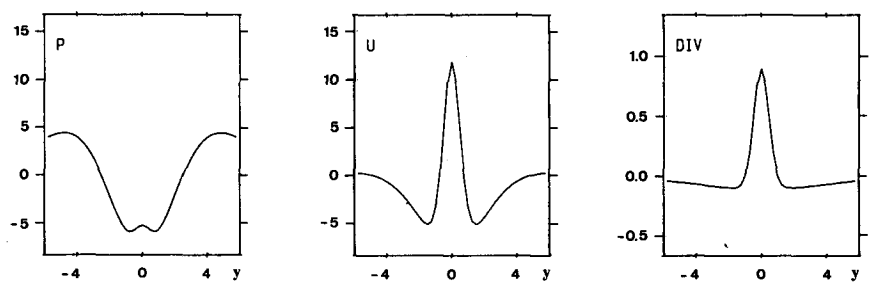

FIG. 3. Meridional midbasin ($x = 20$) section for the flow shown in Fig. 2. Shown are the pressure (left), the zonal velocity (center), and the boundary layer divergence forcing the flow (right). Damping constant $\epsilon = 0.01$.

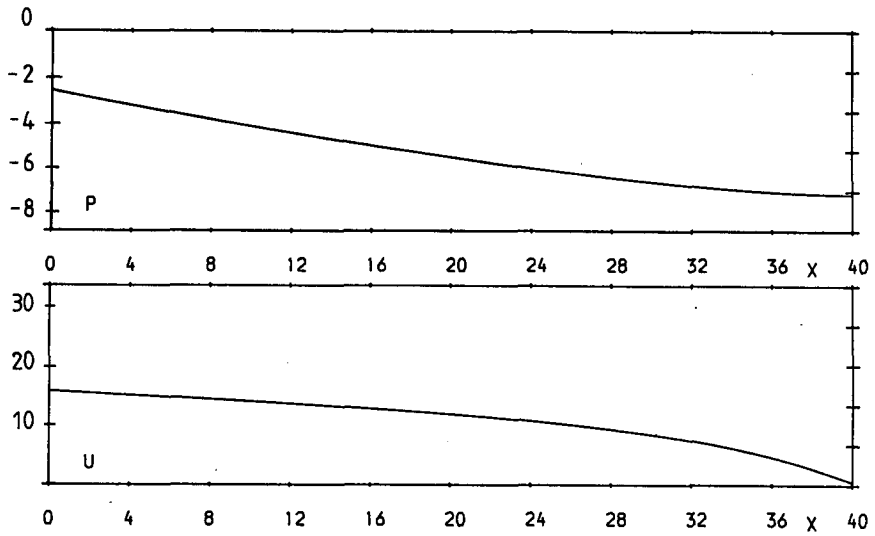

FIG. 4. Zonal section along the equator for the flow shown in Fig. 2. Shown are the pressure (top) and the zonal velocity (above).

wind off the equator, as discussed by Gill (1982) and as found in the model of McCreary (1981).

The other interesting question is whether a narrow band of divergence some distance north of the equator can cause the equatorial countercurrent and the associated pressure trough. To model this situation we force the model with a narrow divergence distribution located four Rossby radii north of the equator, and equal and opposite but broadly distributed convergence,

$$W_E = \frac{1}{15}\left\{3D_0[3(y-4)] - \frac{1}{3}D_0(y/3)\right\} \qquad (37)$$

for which the coefficients W_n can again be computed using (19). Note that the divergence is only one-fifth of that used in the symmetric case of Figs. 2, 3 and 4. The flow, shown in Fig. 8, was computed using the same damping, $\epsilon = 0.01$, as for the symmetric and antisymmetric cases. One finds a trough at the latitude of the divergence, with eastward currents on the southern side of the trough, and somewhat weaker westward currents on the northern side.

Finally, the three cases studied above are combined as a rough representation of the situation one might expect to find in the Pacific Ocean. The flow shown in

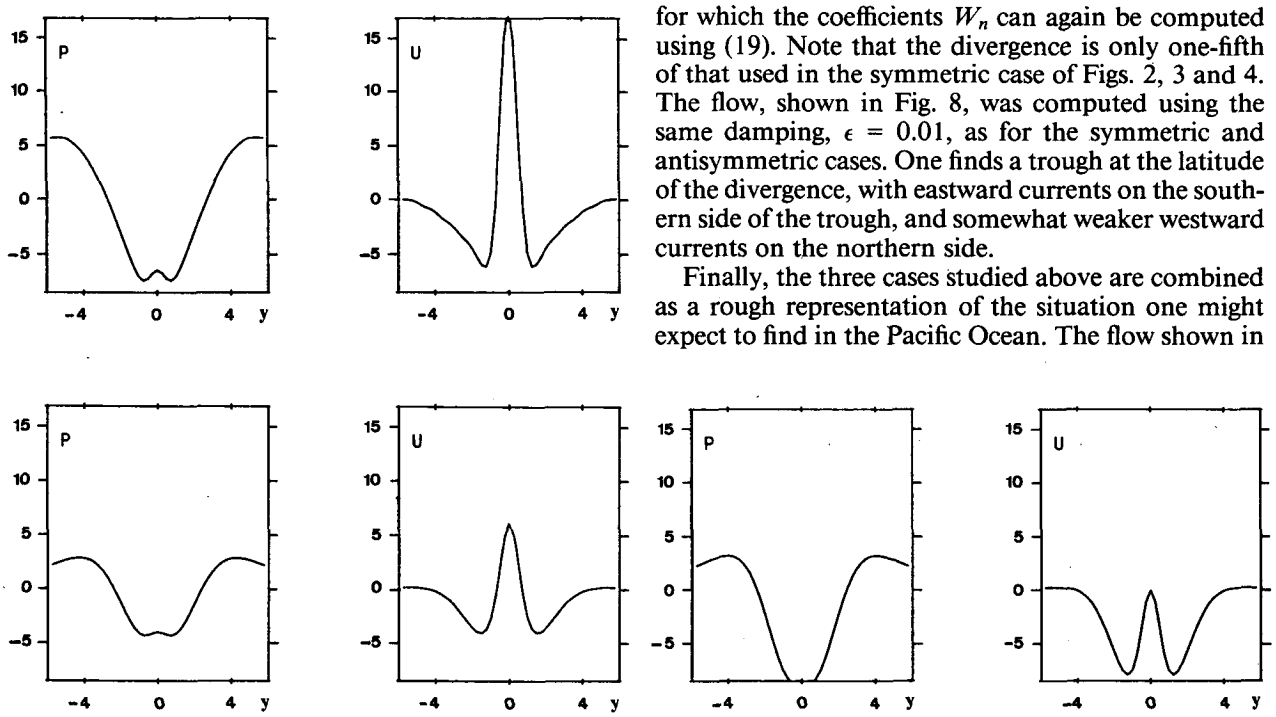

FIG. 5. Meridional midbasin sections for the same forcing as in Figs. 2, 3 and 4, but with weaker damping $\epsilon = 0.005$ (top), and stronger damping $\epsilon = 0.02$ (above). Pressure on the left and zonal velocity on the right should be compared with Fig. 3 where $\epsilon = 0.01$.

FIG. 6. Solution in the absence of basin boundaries. The pressure (left) and zonal velocity (right) are computed for the same forcing as in Figs. (2)–(5) and with a damping constant $\epsilon = 0.02$ (see Fig. 5, bottom).

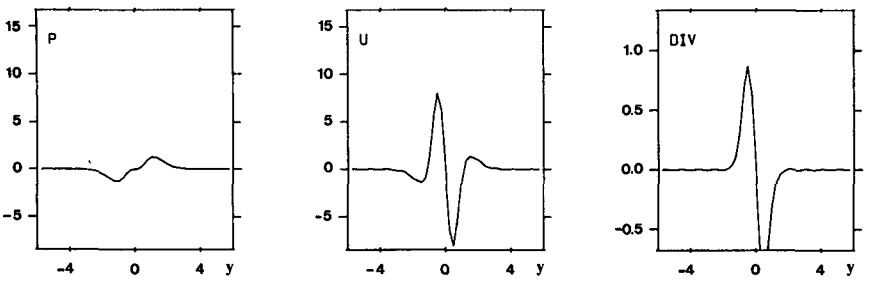

FIG. 7. Meridional midbasin sections for forcing asymmetric about the equator. Shown are the pressure (left), zonal velocity (center), and boundary layer divergence (right). Damping constant $\epsilon = 0.01$.

Fig. 9 thus corresponds to large-scale easterly winds, with a southerly component at the equator, and an intertropical convergence zone near 10°N. One finds an eastward equatorial undercurrent, weaker westward currents to the north and south, and an equatorial countercurrent near 10°N, in good general agreement with the observed current structure. If the pressure distribution is compared with maps of dynamic height of the sea surface relative to 1000 db for the Pacific Ocean (Reid and Arthur, 1975, Wyrtki, 1975) one finds remarkably good qualitative agreement. In the Southern Hemisphere tropics there is a large ridge, sloping down towards the east. By comparison the equatorial band is a trough with a tiny ridge right on the equator. In the Northern Hemisphere is a second ridge between the equator and the intertropical convergence zone, another trough at the ITCZ, and another ridge poleward of it.

6. Analytic solution for undamped equatorial waves

We shall now study the solution when the damping of the long waves vanishes. This inviscid solution is useful not only because it shows what tends to happen as the wave damping becomes small, but also because it will make it possible to compare the present model with a commonly used model in which the effect of the wind appears as a body force. In the limit of vanishing wave damping the model (7)–(9) becomes, in the steady state,

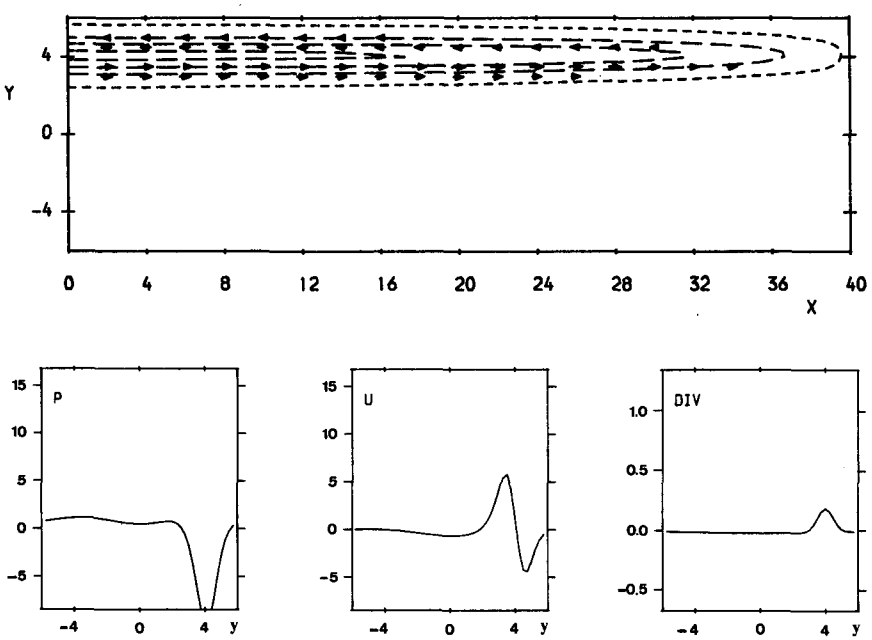

FIG. 8. Solution for a zonally symmetric band of boundary layer divergence centered four Rossby radii north of the equator, with weak, broadly spread, convergence. The divergence forcing is only one-fifth as strong as in Fig. 2. Damping constant $\epsilon = 0.01$. The boundary layer divergence causes a trough in the ocean pressure field, with an eastward equatorial countercurrent to the south.

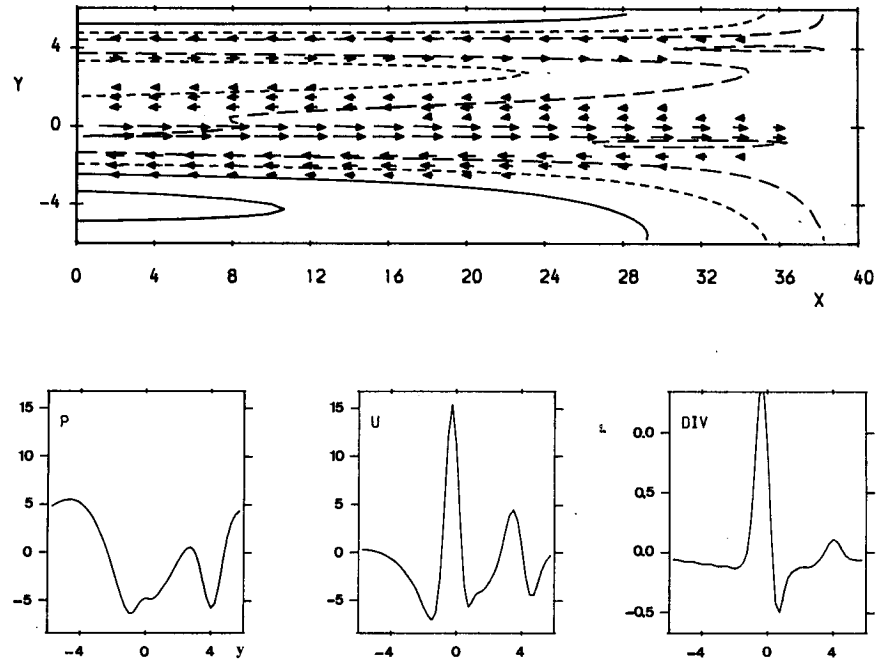

FIG. 9. Solution for the combined forcings of Figs. 2, 7 and 8. The flow is due to the combined effects of a large-scale easterly wind, a southerly component at the equator, and an intertropical convergence zone near 10°N. The damping constant is $\epsilon = 0.01$. There is a strong eastward undercurrent shifted slightly south of the equator, and an eastward equatorial countercurrent near $y = 4$. Elsewhere the flow is fairly weak and westward.

$$-\frac{1}{2}yv = -\partial\phi/\partial x, \quad \frac{1}{2}yu = -\partial\phi/\partial y$$

$$\partial u/\partial x + \partial v/\partial y = -W_E \tag{38}$$

with an eastern boundary at $x = 0$ and a western boundary at $x = L$. At the eastern boundary we require the zonal velocity to be zero, at the western boundary the total zonal mass flux must be zero. The solution to this set of equations was given by Cane and Sarachik (1977), although with a different interpretation. The solution for u, v and ϕ may be written

$$u = M(y)(x-L), \quad v = N(y), \quad \phi = P(y)(x-L) + P_0 \tag{39}$$

in the case where W_E is independent of x, and

$$M(y) = -(2W_E + y dW_E/dy)$$

$$N(y) = yW_E$$

$$P(y) = \frac{1}{2}y^2 W_E. \tag{40}$$

We shall now compute a specific solution for the fundamental problem of a uniform zonal wind blowing over a tropical ocean. We need a simple model of the boundary layer mass flow, which reproduces the two important features that the mass flow is downwind at the equator where the Coriolis forces vanish, and perpendicular to the wind at high latitudes where the Coriolis forces are important. The simplest model with these features has a three-way balance of forces between the wind stress, the Coriolis forces, and a simple drag law. The x and y momentum equations for this boundary layer model are

$$\delta U - \frac{1}{2}yV = \tau, \quad \delta V + \frac{1}{2}yU = 0 \tag{41}$$

where τ is the zonal wind stress, and has the solution

$$U = \frac{1}{1+Y^2}\frac{\tau}{\delta}, \quad V = \frac{-Y}{1+Y^2}\frac{\tau}{\delta} \tag{42}$$

in terms of the scaled variable $Y = y/2\delta$. At the equator the mass flux is downwind and its amount inversely proportional to δ. At high latitudes, here defined as $Y^2 \gg 1$, we have the Ekman solution of flow at right angle to the wind and independent of δ, which may be seen by writing V as

$$V = -\frac{2\tau}{y}\left(1 - \frac{1}{1+Y^2}\right). \tag{43}$$

The boundary layer divergence dV/dy is shown in Fig. 10, and is very similar in shape to that used in the viscous model (Fig. 3).

With this boundary-layer model the interior flow is given by

$$M(y)=\frac{1-2Y^2-Y^4}{(1+Y^2)^3}\tau/\delta^2$$

$$N(y)=-Y\left[\frac{1-Y^2}{(1+Y^2)^2}\right]\tau/\delta$$

$$P(y)=-Y^2\left[\frac{1-Y^2}{(1+Y^2)^2}\right]\tau. \quad (44)$$

The functions M and P for the geostrophic zonal flow and the pressure are shown in Fig. 11. One can see that the qualitative features of a meridional section are identical to the viscous model results shown in Fig. 3. We can therefore conclude that the flows and height fields obtained earlier were not artifacts of the particular damping law used, but result fundamentally from the combination of nearly geostrophic flow and forcing by the boundary-layer divergence.

The major difference between the inviscid and the viscous solutions is that whereas in the inviscid solution the zonal currents and the pressure grow linearly as one goes west from the eastern boundary, in the viscous solution the growth rate rapidly diminishes, so that the zonal currents and the pressure are nearly independent of x over a large part of the basin. Near the eastern boundary the two solutions are very similar, and the extent of the region where they are similar will increase as the wave damping decreases.

The asymptotic properties of the solution very close to and very far from the equator are easily obtained from (44). For the zonal velocity field we have

$$Y^2\gg 1, \quad M\sim -\tau/\delta^2Y^2=-4\tau/y^2 \quad (45)$$

$$Y^2\ll 1, \quad M\sim(1-5Y^2)\tau/\delta^2=(1-5y^2/4\delta^2)\tau/\delta^2. \quad (46)$$

Near the equator we have a jet which gets stronger but narrower as δ decreases. At high latitudes there is a return flow which is approximately independent of δ. For the meridional velocity we find

$$Y^2\gg 1, \quad N\sim \tau/\delta Y=2\tau/y \quad (47)$$

$$Y^2\ll 1, \quad N\sim -Y\tau/\delta=-y\tau/2\delta^2. \quad (48)$$

In the inviscid solution the divergence of the meridional geostrophic velocity at the equator has the same sign and magnitude as the divergence of the boundary-layer flow. The compensating convergence of the zonal velocity is therefore twice the boundary-layer divergence. At high latitudes the pressure-driven meridional flow is just minus the boundary-layer flow. For the pressure we find

$$Y^2\gg 1, \quad P\sim\tau \quad (49)$$

$$Y^2\ll 1, \quad P\sim -Y^2\tau=-y^2\tau/4\delta^2. \quad (50)$$

In the case of an easterly wind we find two small dips in the surface level, north and south of the equator. They make it possible for the eastward equatorial jet to be in geostrophic equilibrium. Then as one proceeds to higher latitudes the surface rises, until at high latitudes the surface slope balances the wind stress.

7. Comparison with a model forced by wind stress

We shall compare the present model with a commonly used single-layer model in which the wind stress acts directly upon the flow in the upper layer. In its time-dependent, inviscid form this model has been studied, among others by Lighthill (1969) and Cane and Sarachik (1976, 1977, 1979), and the effects of damping were studied by Yamagata and Philander (1985). We shall study this model in its steady, inviscid form so it can be compared with the inviscid model of the previous section. Using the same notation we have

$$-\frac{1}{2}yv_s=-\partial\phi/\partial x+\tau, \quad \frac{1}{2}yu_s=-\partial\phi/\partial y$$

$$\partial u_s/\partial x+\partial v_s/\partial y=0 \quad (51)$$

for a zonal wind. The velocities u_s and v_s are to be interpreted as vertical mean velocities in the upper layer. Cane and Sarachik (1977) have shown that for a uniform wind the solution of (51) has zero currents and a balance between the tilt of the surface and the wind stress,

$$u_s=v_s=0, \quad \partial\phi/\partial x=\tau. \quad (52)$$

This model is clearly unsatisfactory as it misses out the most striking feature of the equatorial circulation, namely the strong equatorial current and the weaker return flows to the north and south. Moreover, the height field is not very good either as it gives a surface slope independent of latitude, whereas the present model and the observations for the Pacific Ocean show that the height is much lower in a band of latitudes about the equator.

As the stress-forcing model is often very valuable and is commonly used, it is of interest to examine its relation to the present model and to see why it is less successful for the equatorial ocean. The obvious area of application of the single-layer, stress-forcing model is in cases where all properties are fairly uniform throughout depth of the layer, for example storm surges in shallow, well-mixed seas. This does not apply in the equatorial ocean. It is true that the pressure is nearly uniform in the upper layer, but the velocities are strongly sheared and nonuniform, as sketched in Fig. 1, indicating that there is a surface boundary layer. This in turn indicates indirectly that the wind stress is taken up nonuniformly in the upper layer.

In cases where there is a surface boundary layer the stress-forcing model can still be very useful provided the mass flux in the boundary layer satisfies a special condition, namely, that it satisfies the Ekman relation. We can show this very simply by dividing the total flow u_s, v_s in (51) into a geostrophic flow u, v and a boundary layer flow V, satisfying

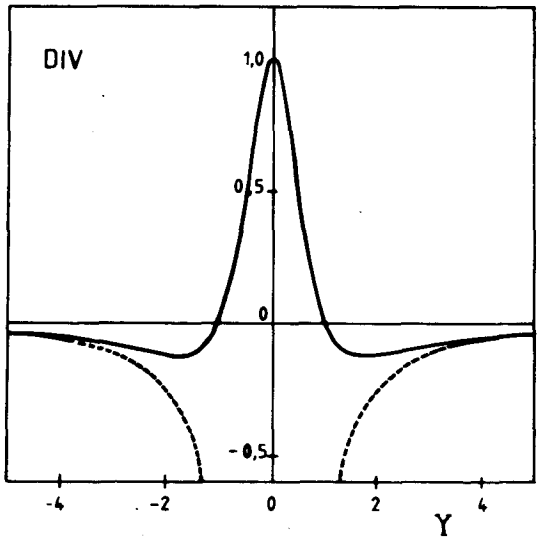

FIG. 10. The divergence of the boundary layer flow, $-2\delta^2(dV/dy)/\tau$, for an easterly wind and the simple boundary layer model developed in section 6. The flow is divergent in a narrow region centered on the equator, and convergent polewards. The dashed curve shows the divergence that would be found if the boundary-layer flow was governed by the Ekman relation. The two models are equivalent at higher latitudes, but near the equator the Ekman relation gives unrealistic convergence.

$$\left.\begin{aligned} -\frac{1}{2}yv = -\partial\phi/\partial x, \quad \frac{1}{2}yu = -\partial\phi/\partial y \\ \partial u/\partial x + \partial v/\partial y = -\partial V/\partial y \end{aligned}\right\} \tag{53}$$

$$V = -2\tau/y. \tag{54}$$

The stress-forcing model is thus equivalent to the boundary-layer divergence model, provided the boundary-layer mass flux is given by the Ekman relation. In midlatitudes, where this is the case, the two formulations are equivalent, and the original paper by Stommel (1948) on the midlatitude circulation, for example, was in the stress formulation.

In the equatorial ocean the Ekman relation does not provide a good description of the boundary-layer mass flux, and we cannot, therefore, expect the two models to be equivalent. If we compare the stress model (53), (54) with the inviscid boundary-layer divergence model (38), (43), we see that the only difference between them lies in the form of the boundary-layer mass flux. The simple model of section 6 reproduces the main features of the observed boundary-layer divergence, whereas the Ekman relation does not (Fig. 10). The observed boundary-layer divergence for an easterly wind is strongly divergent in a narrow region centered on the equator and convergent polewards, whereas the Ekman flux is everywhere convergent, infinitely so at the equator.

It might be argued that the stress formulation model could be valid in the equatorial ocean by accommodating two different balances: a balance between stress and Ekman flux away from the equator, and a balance between stress and pressure gradient near the equator. That this does not happen in reality is amply demonstrated by the fact that the model misses the equatorial-current field completely, and does not provide a good description of the pressure field either. The wind-stress model solution is perhaps best thought of as the outer-limit component of the inviscid boundary-layer

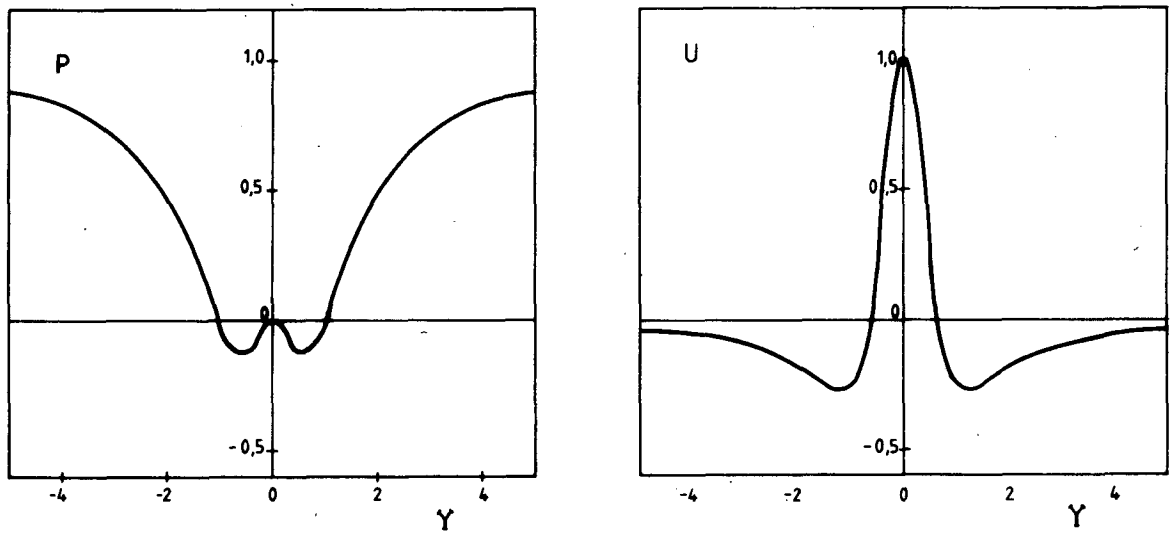

FIG. 11. Meridional sections of pressure (left, $P(y)/\tau$) and zonal velocity (right, $\delta^2 M(y)/\tau$) for the undamped analytic model of section 6 with the forcing of Fig. 10. The sections are very similar to those for the damped model, shown in Fig. 3. With an easterly wind there is a narrow eastward equatorial current and weaker westward currents to the north and south. In the undamped model the pressure has the same value on the equator as along the western boundary. At high latitudes $P/\tau \to 1$, so that the surface slope balances the wind stress.

divergence model presented in the previous section. The Ekman flux divergence tends to the model's divergence at large Y (Fig. 10), and similarly the stress formulation solution corresponds to the large y limits (47) and (49) of the boundary layer divergence model: surface slope balancing the stress, and geostrophic meridional flow balancing the meridional Ekman flow.

8. Conclusion

In this paper we have presented and discussed a conceptual model of the wind-driven circulation in the upper tropical oceans. The conceptual model is that the subsurface currents and the pressure field are nearly in geostrophic balance, and are driven by the divergence of the surface boundary layer flow. Given a very simplified representation of the forcing, the simple, linear, analytic model is able to reproduce the gross features of the current and pressure fields. Since it is possible to describe the gross features of the tropical circulation without invoking nonlinearity, particular damping laws, or thermodynamic effects, we conclude that these effects may be important if a detailed representation of the circulation is required, but are not of fundamental importance in understanding the basic flow.

The proposed conceptual model for the upper tropical oceans is, of course, just that which is thought to govern the midlatitude oceans. It would appear, therefore, that a single conceptual model may help to understand and describe both the midlatitude and the tropical oceans.

REFERENCES

Abramowitz, M., and I. A. Stegun, 1965: *Handbook of Mathematical Functions,* Dover, 1046 pp.

Cane, M. A., 1979a: The response of an equatorial ocean to simple wind stress patterns: I Model formulation and analytic results. *J. Mar. Res.,* **37,** 233–252.

——, 1979b: The response of an equatorial ocean to simple wind stress patterns: II Numerical results. *J. Mar. Res.,* **37,** 253–299.

——, and E. S. Sarachik, 1976: Forced baroclinic ocean motions. I. The linear equatorial unbounded case. *J. Mar. Res.,* **34,** 629–664.

——, and ——, 1977: Forced baroclinic ocean motions. II. The linear equatorial bounded case. *J. Mar. Res.,* **35,** 395–432.

——, and ——, 1979: Forced baroclinic ocean motions. III. The linear equatorial basin case. *J. Mar. Res.,* **37,** 355–398.

Gill, A. E., 1975: Models of equatorial currents. *Proc. Symp. on Numerical Models of Ocean Circulation.* Washington, D.C., Natl. Acad. Sci., 364 pp.

——, 1980: Some simple solutions for heat-induced tropical circulation. *Quart. J. Roy. Meteor. Soc.,* **106,** 447–462.

——, 1982: *Atmosphere-Ocean Dynamics.* Academic Press, 662 pp.

——, and A. J. Clarke, 1974: Wind-induced upwelling, coastal currents and sea-level changes. *Deep Sea Res.,* **21,** 325–345.

——, and P. J. Phlips, 1986: Nonlinear effects on heat-induced circulations of the tropical atmosphere. *Quart. J. Roy. Meteor. Soc.,* **112,** 69–91.

Heckley, W. A., and A. E. Gill, 1984: Some simple analytical solutions to the problem of forced equatorial long waves. *Quart. J. Roy. Meteor. Soc.,* **110,** 203–217.

Lighthill, M. J., 1969: Dynamic response of the Indian Ocean to onset of the Southwest Monsoon. *Phil. Trans. Roy. Soc. London,* **A265,** 45–92.

McCreary, J. P., 1981: A linear stratified ocean model of the equatorial undercurrent. *Phil. Trans. Roy. Soc. London,* **A298,** 603–635.

McPhaden, M. J., 1981: Continuously stratified models of the steady state equatorial ocean. *J. Phys. Oceanogr.,* **11,** 337–354.

Philander, S. G. H., and R. C. Pacanowski, 1980: The generation of equatorial currents. *J. Geophys. Res.,* **85,** 1123–1136.

Phlips, P. J., and A. E. Gill, 1987: An analytic model of the heat-induced tropical circulation in the presence of a mean wind. *Quart. J. Roy. Meteor. Soc.,* **113,** 213–236.

Reid, J. L., and R. S. Arthur, 1975: Interpretation of maps of geopotential anomaly for the deep Pacific Ocean. *J. Mar. Res.,* **33**(Suppl.), 37–52.

Stommel, H., 1948: The westward intensification of wind-driven ocean currents. *Trans. Amer. Geophys. Union,* **29,** 202–206.

Wyrtki, K., 1975: Fluctuations of the dynamic topography in the Pacific Ocean. *J. Phys. Oceanogr.,* **5,** 450–459.

——, and G. Meyers, 1976: The trade-wind field over the Pacific Ocean. *J. Appl. Meteor.,* **15,** 698–704.

Yamagata, T., and S. G. H. Philander, 1985: The role of damped equatorial waves in the oceanic response to winds. *J. Oceanogr. Soc. Japan,* **41,** 345–357.